JACS
JOURNAL OF THE AMERICAN CHEMICAL SOCIETY

Communication

pubs.acs.org/JACS

Structure and Morphology of Charged Graphene Platelets in Solution by Small-Angle Neutron Scattering

Emily M. Milner,[†,⊥] Neal T. Skipper,*[,†] Christopher A. Howard,[†] Milo S. P. Shaffer,[‡] David J. Buckley,[†] K. Adam Rahnejat,[†] Patrick L. Cullen,[†] Richard K. Heenan,[§] Peter Lindner,[∥] and Ralf Schweins[∥]

[†]London Centre for Nanotechnology and Department of Physics and Astronomy, University College London, Gower Street, London WC1E 6BT, U.K.

[‡]London Centre for Nanotechnology and Department of Chemistry, Imperial College London, South Kensington Campus, London SW7 2AZ, U.K.

[§]ISIS, Science and Technology Facilities Council, Rutherford Appleton Laboratory, Harwell Science and Innovation Campus, Didcot OX11 0QX, U.K.

[∥]Institut Laue-Langevin, BP 156, 6 rue Jules Horowitz, 38042 Grenoble Cedex 9, France

Supporting Information

ABSTRACT: Solutions of negatively charged graphene (graphenide) platelets were produced by intercalation of nanographite with liquid potassium−ammonia followed by dissolution in tetrahydrofuran. The structure and morphology of these solutions were then investigated by small-angle neutron scattering. We found that >95 vol % of the solute is present as single-layer graphene sheets. These charged sheets are flat over a length scale of >150 Å in solution and are strongly solvated by a shell of solvent molecules. Atomic force microscopy on drop-coated thin films corroborated the presence of monolayer graphene sheets. Our dissolution method thus offers a significant increase in the monodispersity achievable in graphene solutions.

Graphene was first experimentally isolated in 2004,[1,2] although it had been studied theoretically since approximately 60 years earlier.[3] This material is of immense interest as one of the few known two-dimensional (2D) materials, providing free-standing atomic crystals with extraordinary physical properties and potential applications.[4] Graphene sheets have been isolated by micromechanical cleavage of bulk graphite,[1] epitaxial growth from chemical vapor deposition of hydrocarbons,[5,6] and thermal decomposition of SiC.[7] However, these methods are low-yielding and labor-intensive, rendering them less than ideal for industrial scale-up. For this reason, there is great interest in graphene production/manipulation via liquid-phase routes,[8] which can be used for the scalable production of functional films and composites. Current methods include the dispersion of graphite powders in organic solvents via sonication,[9−11] solvothermal synthesis,[12,13] polymer and surfactant wrapping,[14,15] and reduction of soluble graphite oxides.[16−21] Higher concentrations of dispersed material (up to 2 mg/mL) can be achieved by protonation of graphite in chlorosulfonic acid[22] or thermal exfoliation and treatment in oleum.[23] Another approach is to start with graphite intercalation compounds (GICs), which are formed by inserting arrays of atoms or molecules between the graphene sheets of graphite.[24−26] GICs such as those based on potassium are soluble after stirring or sonication to ∼0.7 mg/mL in *N*-methylpyrrolidone[27] and other aprotic organic solvents[28] and can be exfoliated in ethanol and then dissolved in 1,2-dichlorobenzene.[29] In addition to the increased concentration of pristine (unfunctionalized) graphene, GIC starting materials have the further advantage of potentially providing some control over the solution-phase speciation, to yield a predominance of mono-, bi- or trilayer graphene.[27,28,30] Nevertheless, layer thickness polydispersity remains a key issue in liquid-phase processing of graphene, with current production methods producing a mixture of one-, two-, and three-layer or higher graphenes.[8,31]

In this paper, we present a two-stage route for graphene dissolution, as illustrated schematically in Figure 1. First, potassium−ammonia solution is intercalated into nanographite fibers. The resultant potassium−ammonia GICs then dissolve in tetrahydrofuran (THF) to form solutions of negatively charged graphene, which hereafter we will call "graphenide" to indicate the anionic and discrete character of this species.[32] Using a combination of small-angle neutron scattering (SANS), Monte Carlo computer simulations, atomic force microscopy (AFM), and Raman spectroscopy, we show that the predominant solute species (>95 vol %) is strongly solvated monolayer graphenide platelets.

Graphene platelets with diameters in the range 100−250 nm were intercalated by immersion in potassium−ammonia solutions to produce expanded intercalates with the approximate composition $KC_{48}(NH_3)_4$.[33,34] Following the removal of excess ammonia, these GICs were dissolved in THF-d_8 by very brief and mild bath sonication (section S1 in the Supporting Information). Solutions were prepared at 0.1 and 0.01 wt % GIC (corresponding to ∼1 and ∼0.1 mg/mL respectively), at which concentrations full dissolution into monolayer graphene sheets would correspond to the dilute-solute limit.[35] SANS data were collected over a Q range of ∼0.005 to 0.3 $Å^{-1}$ using the D11 instrument at the Institut Laue Langevin, Grenoble

Received: December 30, 2011
Published: May 10, 2012

dx.doi.org/10.1021/ja211869u | *J. Am. Chem. Soc.* 2012, 134, 8302−8305

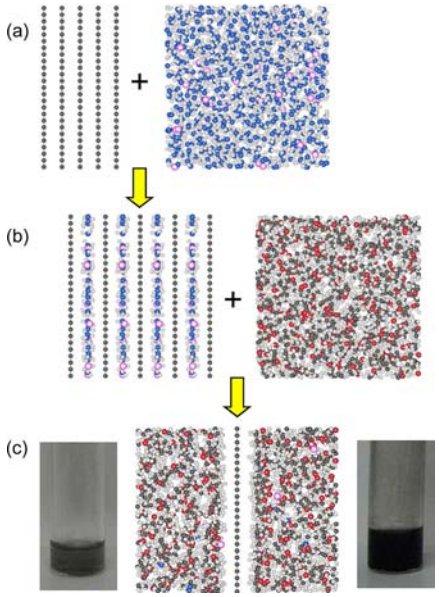

Figure 1. Schematic of our two-stage graphene dissolution process: (a) Graphite (left) is intercalated with potassium−ammonia solution (right) to yield (b) graphite−potassium−ammonia $KC_{48}(NH_3)_4$ (left) with an expanded layer spacing of ∼6.4 Å. $KC_{48}(NH_3)_4$ dissolves in THF (right). (c) Solvated charged graphenide sheet in THF (center), with photos of a 0.01 wt % solution (left) and a 0.1 wt % solution (right). Atomic color scheme: K, pink; H, light-gray; N, blue; O, red; C, dark-gray.

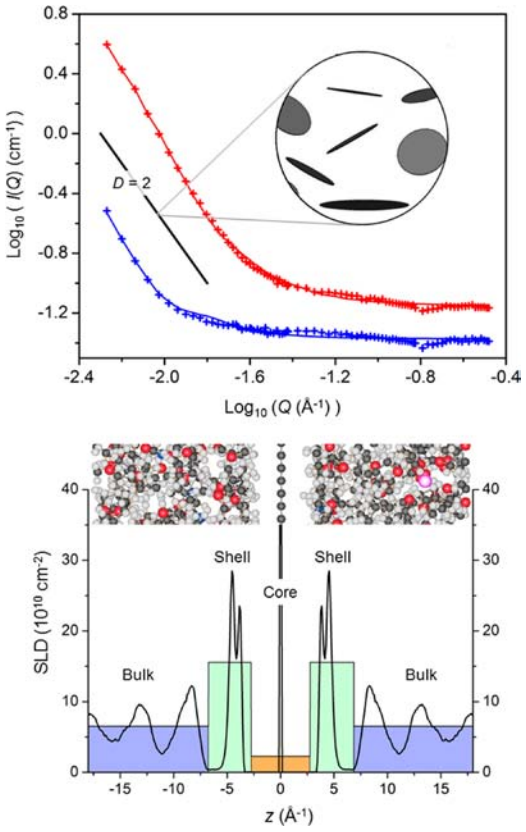

Figure 2. Small-angle neutron scattering from graphenide platelets in solution. (a) Solvent-corrected SANS data (represented by points) and fits (lines) for $KC_{48}(NH_3)_n$ in D_8-THF at GIC concentrations of 0.1 wt % (red) and 0.01 wt % (blue). The level of the 0.01 wt % data plot has been increased by 1 to improve visibility. The solid black line shown has a gradient $D = 2$ as expected for a solution of randomly oriented thin discs of approximate minimum radius 150 Å, as illustrated in the schematic. (b) Scattering length density (SLD) normal to the *ab*-plane of a single charged graphene platelet in ammonia − D_8-THF as obtained by Monte Carlo simulation, with the "core-shell-bulk" model used in the fit shown in Figure 2a illustrated schematically as the solid blocks (color scheme: Core − orange, Shell − green, Bulk − blue), and a representative molecular configuration above (atomic color scheme: K − pink, H − light gray, N − blue, O − red, C − dark gray).

(section S2). SANS is potentially a very powerful technique for probing the structure and morphology of graphenes in solution,[35,36] as has been demonstrated for example by studies of laponite clay discs in aqueous media.[37,38] Specifically, SANS can be used to determine whether the graphene is present as single-layer or more agglomerated species as well as the graphene morphology (e.g., flat, rippled, or folded) and the solvation structure.[36,39] At intermediate Q values, the SANS intensity $I(Q)$ is proportional to Q^{-D}, where $Q = (4\pi \sin\theta)/\lambda$ is the magnitude of the scattering wave vector and D is the fractal exponent of the scattering objects.[40] The expected fractal exponent of fully dispersed platelike objects is $D \approx 2$.[37,38] Dispersions containing larger agglomerates or scrolled or folded graphenes, on the other hand, are usually dominated by surface fractals, typically with $D = 3$−4.[40]

In Figure 2, we show the SANS patterns from our samples. Over the low-Q region of our data, the gradients of these plots fall in the approximate range −1.8 to −2.4 as Q decreases, giving average D values of 2.2 ($\log_{10} Q < -1.6$) and 2.1 ($\log_{10} Q < -2.0$) for the 0.1 and 0.01 wt % solution, respectively. These gradients are consistent with 2D platelets as the dominant scatterers but indicate also the presence of some objects with larger fractal exponents at both concentrations.[35,40] To examine the data in more detail, the SANS patterns for the two concentrations were fitted to scattering from discs/cylinders using the program FISH (section S2).[41,42] The best fits, shown in Figure 2a, necessitated the inclusion of two distinct types of scattering objects in the model: (1) thin solvated "core−shell−bulk" discs of approximate core thickness 5−6 Å (0.5−0.6 nm) and apparent radius 150 Å (15 nm) and (2) cylindrical stacks of approximate height 300 Å (30 nm) and minimum radius 1250 Å (125 nm). We assign type-1 to single solvated graphenide sheets and take type-2 as evidence for short segments of graphite fibers that were not successfully exfoliated because of incomplete intercalation or defects that bind the layers together. The absence of an $I(Q) \propto Q^{-4}$ Porod regime at high Q is consistent with the presence of type-1 thin discs,[38] while the onset of the Guinier regime at low Q is outside our instrumental window since it would be expected only for $Q < 2\pi/R_2$ (where $R_2 = 1250$ Å is the minimum radius of the type-2 stacks).[35] The fits indicate that objects of type 1 are by far the dominant species over the concentration range studied here, accounting for >95 vol % of the scatterers.

To calculate the SANS expected from single-layer graphenide and to compare with the best-fit model, we conducted a classical Monte Carlo simulation of a single sheet of $KC_{48}(NH_3)_2$ in THF-d_8 (section S3). The simulated neutron scattering length density (SLD) normal to the graphene is shown in Figure 2b. This calculation indicates that a single graphene sheet has an effective *core* thickness of ∼5.3 Å in solution, in excellent agreement with the best-fit value of 5.6 Å obtained from our fits to the SANS data. Moreover, as noted in simulations of other solvents,[43] we found a strong solvation

dx.doi.org/10.1021/ja211869u | J. Am. Chem. Soc. 2012, 134, 8302−8305

shell with an approximate thickness of 4.2 Å around each graphenide platelet. Again, this value is in excellent agreement with that obtained from our experimental fit (4.5 Å). It is also clear from the simulations that the THF solvent shell forms hydrogen bonds to the graphenide sheets, since H atoms are found closest to the surfaces (see the light-gray-colored H atoms in Figures 1c and 2b). This observation is consistent with structural studies of the solvation of fulleride[44,45] and nanotubide[46] anions. One would expect partial condensation of potassium cations onto the graphenide surface,[47] but unfortunately, we could not estimate this proportion from our data because the average SLD of potassium (and ammonia) in our solutions was only ∼1% of the average SLD of the graphenide.

The apparent radius of ∼150 Å for the type-1 graphene discs indicates the extent over which the solvated graphenide may be viewed as rigid (rather than rippled) within the limits of the core thickness of 5 Å. In suspended graphene, typical surface curvatures of 5° are observed with corrugations of spatial extent $L \leq 250$ Å (i.e., amplitudes of 10−20 Å).[48,49] We therefore conclude that the amplitude of the corrugations in our solvated graphenide is significantly less than that for graphene suspended in vacuo, presumably as a result of the effects of charging of the surface and concomitant Coulomb repulsion.[22]

To complement the SANS data, AFM was performed on graphene films formed by drop-coating our solutions onto mica in an inert atmosphere. Deflection images obtained in contact mode clearly show islands of graphene (Figure 3a). The height profile of the line scan (Figure 3b) shows that these islands are ∼1 nm high, which is typical of those reported for monolayer graphene.[1,14,23,28] Moreover, statistical analysis over a 2 μm × 2 μm square gave an average feature height of 0.93 nm with a standard deviation of 0.2 nm (Figure 3c). The widths of these platelets are on the order of 100−250 nm, which is comparable to the diameter of the pristine nanographite platelet fibers found using SEM (section S1) and also consistent with the diameters of the type-2 species obtained from our fits to the SANS data. The presence of monolayer graphene species was further supported by Raman spectroscopy studies of platelets deposited from solution (section S4).

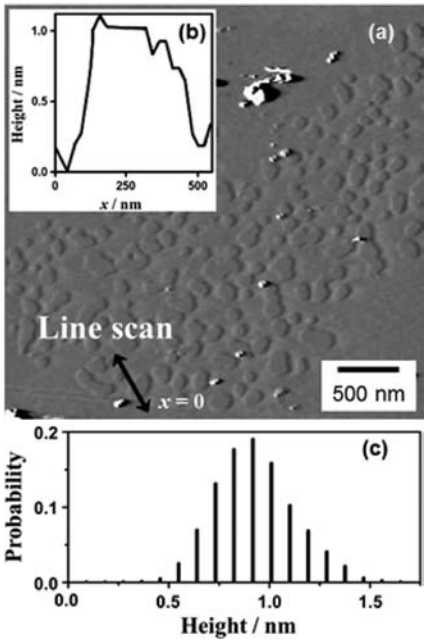

Figure 3. AFM of nanographene solutions drop-coated onto mica. (a) Typical contact-mode deflection image of deposited nanographene in which individual platelets with dimensions of 100−250 nm are clearly visible. (b) Typical line-scan height profile of the same sample showing that the nanographene layers are ∼1 nm high. The white particles are thought to be potassium (hydr)oxide particles. (c) Statistical analysis of feature heights over a 2 μm × 2 μm area of the surface, which was chosen for the absence of white particles. The average feature height was found to be 0.93 nm with standard deviation of 0.2 nm.

In conclusion, we have presented a two-stage route for graphene dissolution in which first potassium−ammonia is intercalated into graphite and then this salt is dissolved in THF. In situ SANS, a very powerful technique for probing the structure and morphology of graphenes in solution, showed that >95 vol % of the dissolved solute is present as strongly solvated single-layer graphenide sheets, which are flat and rigid over a radius of ∼150 Å. The presence of single graphene sheets was confirmed ex situ using AFM and Raman spectroscopy of drop-coated films. It is likely that ammonia plays a key role in the efficiency of the process, since it readily produces an expanded starting material and strongly solvates the interlayer potassium cations.[24,34] The dissolution of graphenide would then be driven by the entropic contribution of the dissociated cations, which leads to electrostatic repulsion between the graphenide. The degree of counterion dissociation and condensation has been discussed in the light of polyelectrolyte theory for the case of nanotubides,[47] and a future extension of this theory to the present 2D graphenide case would be instructive. In addition, the starting material consists of laterally defined single crystals, without grain boundary constraints that may limit conventional graphite material processing. A striking finding is that the size and shape of the original graphitic discs appears to be retained during the dissolution, suggesting a means to produce dispersions of monodispersed graphenes if the starting material is suitably controlled.

■ ASSOCIATED CONTENT

Supporting Information

Starting material and sample preparation, SANS, Monte Carlo computer simulations, and Raman spectroscopy. This material is available free of charge via the Internet at http://pubs.acs.org.

■ AUTHOR INFORMATION

Corresponding Author

n.skipper@ucl.ac.uk

Present Address

[⊥]Faculty of Engineering, The University of Nottingham, University Park, Nottingham NG7 2RD, U.K. (E.M.M.).

Notes

The authors declare no competing financial interest.

■ ACKNOWLEDGMENTS

This work was funded by the EPSRC and BOC Linde. The authors thank David Bowyer at the ILL and Kevin Lee at UCL. They also thank Ann Terry at ISIS for help with preliminary SANS experiments on LOQ and Richard Winchester for assistance with transmission electron microscopy.

REFERENCES

(1) Novoselov, K. S.; Geim, A. K.; Morozov, S. V.; Jiang, D.; Zhang, Y.; Dubonos, S. V.; Grigorieva, I. V.; Firsov, A. A. *Science* **2004**, *306*, 666.
(2) Geim, A. K.; Novoselov, K. S. *Nat. Mater.* **2007**, *6*, 183.
(3) Wallace, P. R. *Phys. Rev.* **1947**, *71*, 622.
(4) Editorial: Graphene 2.0. *Nat. Nanotechnol.* **2008**, *3*, 517.
(5) Cai, W.; Moore, A. L.; Zhu, Y.; Li, X.; Chen, S.; Shi, L.; Ruoff, R. S. *Nano Lett.* **2010**, *10*, 1645.
(6) Li, X.; Cai, W.; An, J.; Kim, S.; Nah, J.; Yang, D.; Piner, R.; Velamakanni, A.; Jung, I.; Tutuc, E.; Banerjee, S. K.; Colombo, L.; Ruoff, R. S. *Science* **2009**, *324*, 1312.
(7) Berger, C.; Song, Z.; Li, T.; Li, X.; Ogbazghi, A. Y.; Feng, R.; Dai, Z.; Marchenkov, A. N.; Conrad, E. H.; First, P. N.; de Heer, W. A. *J. Phys. Chem. B* **2004**, *108*, 19912.
(8) Green, A. A.; Hersam, M. C. *J. Phys. Chem. Lett.* **2010**, *1*, 544.
(9) Hernandez, Y.; Nicolosi, V.; Lotya, M.; Blighe, F. M.; Sun, Z.; De, S.; McGovern, I. T.; Holland, B.; Byrne, M.; Gun'ko, Y. K.; Boland, J. J.; Niraj, P.; Duesberg, G.; Krishnamurthy, S.; Goodhue, R.; Hutchinson, J.; Scardaci, V.; Ferrari, A. C.; Coleman, J. N. *Nat. Nanotechnol.* **2008**, *3*, 563.
(10) Kozhemyakina, N. V.; Englert, J. M.; Yang, G.; Spiecker, E.; Schmidt, C. D.; Hauke, F.; Hirsch, A. *Adv. Mater.* **2010**, *22*, 5483.
(11) Hernandez, Y.; Lotya, M.; Rickard, D.; Bergin, S. D.; Coleman, J. N. *Langmuir* **2010**, *26*, 3208.
(12) Choucair, M.; Thordarson, P.; Stride, J. A. *Nat. Nanotechnol.* **2009**, *4*, 30.
(13) Qian, W.; Hao, R.; Hou, Y.; Tian, Y.; Shen, C.; Gao, H.; Liang, X. *Nano Res.* **2009**, *2*, 706.
(14) Lotya, M.; Hernandez, Y.; King, P. J.; Smith, R. J.; Nicolosi, V.; Karlsson, L. S.; Blighe, F. M.; De, S.; Wang, Z.; McGovern, I. T.; Duesberg, G. S.; Coleman, J. N. *J. Am. Chem. Soc.* **2009**, *131*, 3611.
(15) Liang, Y. T.; Hersam, M. C. *J. Am. Chem. Soc.* **2010**, *132*, 17661.
(16) Park, S.; Ruoff, R. S. *Nat. Nanotechnol.* **2009**, *4*, 217.
(17) Malik, S.; Vijayaraghavan, A.; Erni, R.; Ariga, K.; Khalakhan, I.; Hill, J. P. *Nanoscale* **2010**, *2*, 2139.
(18) Li, D.; Muller, M. B.; Gilje, S.; Kaner, R. B.; Wallace, G. G. *Nat. Nanotechnol.* **2008**, *3*, 101.
(19) Cai, D.; Song, M. *J. Mater. Chem.* **2007**, *17*, 3678.
(20) Niyogi, S.; Bekyarova, E.; Itkis, M. E.; McWilliams, J. L.; Hamon, M. A.; Haddon, R. C. *J. Am. Chem. Soc.* **2006**, *128*, 7720.
(21) Si, Y.; Samulski, E. T. *Nano Lett.* **2008**, *8*, 1679.
(22) Behabtu, N.; Lomeda, J. R.; Green, M. J.; Higginbotham, A. L.; Sinitskii, A.; Kosynkin, D. V.; Tsentalovich, D.; Parra-Vasquez, A. N. G.; Schmidt, J.; Kesselman, E.; Cohen, Y.; Talmon, Y.; Tour, J. M.; Pasquali, M. *Nat. Nanotechnol.* **2010**, *5*, 406.
(23) Li, X.; Zhang, G.; Bai, X.; Sun, X.; Wang, X.; Wang, E.; Dai, H. *Nat. Nanotechnol.* **2008**, *3*, 538.
(24) Solin, S. A.; Zabel, H. *Adv. Phys.* **1988**, *37*, 87.
(25) Dresselhaus, M. S.; Dresselhaus, G. *Adv. Phys.* **2002**, *51*, 1.
(26) Enoki, T.; Suzuki, M.; Endo, M. *Graphite Intercalation Compounds and Applications*; Oxford University Press: New York, 2003.
(27) Catheline, A.; Vallés, C.; Drummond, C.; Ortolani, L.; Morandi, V.; Marcaccio, M.; Iurlo, M.; Paolucci, F.; Pénicaud, A. *Chem. Commun.* **2011**, *47*, 5470.
(28) Vallés, C.; Drummond, C.; Saadaoui, H.; Furtado, C. A.; He, M.; Roubeau, O.; Ortolani, L.; Monthioux, M.; Pénicaud, A. *J. Am. Chem. Soc.* **2008**, *130*, 15802.
(29) Kwon, J.; Lee, S. H.; Park, K.-H.; Seo, D.-H.; Lee, J.; Kong, B.-S.; Kang, K.; Jeon, S. *Small* **2011**, *7*, 864.
(30) Shih, C.-J.; Vijayaraghavan, A.; Krishnan, R.; Sharma, R.; Han, J.-H.; Ham, M.-H.; Jin, Z.; Lin, S.; Paulus, G. L. C.; Reuel, N. F.; Wang, Q. H.; Blankschtein, D.; Strano, M. S. *Nat. Nanotechnol.* **2011**, *6*, 439.
(31) Green, A. A.; Hersam, M. C. *Nano Lett.* **2009**, *9*, 4031.
(32) McCleverty, J. A.; Connelly, N. G. *Nomenclature of Inorganic Chemistry II: Recommendations 2000*; Royal Society of Chemistry: Cambridge, U.K., 2001.
(33) York, B. R.; Solin, S. A. *Phys. Rev. B* **1985**, *31*, 8206.
(34) Walters, J. K.; Skipper, N. T.; Soper, A. K. *Chem. Phys. Lett.* **1999**, *300*, 444.
(35) Chen, S. H. *Annu. Rev. Phys. Chem.* **1986**, *37*, 351.
(36) King, S. M. In *Modern Techniques for Polymer Characterisation*; Pethrick, R. A., Dawkins, J. V., Eds.; Wiley: Chichester, U.K., 1999.
(37) Ramsay, J. D. F.; Lindner, P. *J. Chem. Soc., Faraday Trans.* **1993**, *89*, 4207.
(38) Nelson, A.; Cosgrove, T. *Langmuir* **2004**, *20*, 2298.
(39) Pedersen, J. S. *Adv. Colloid Interface Sci.* **1997**, *70*, 171.
(40) Teixeira, J. J. *Appl. Crystallogr.* **1988**, *21*, 781.
(41) Heenan, R. K. *The "FISH" Reference Manual (Data Fitting Program for Small Angle Diffraction)*; Rutherford Appleton Laboratory: Didcot, U.K., 2005.
(42) Ghosh, R. E.; Egelhaaf, S. U.; Rennie, A. R. *A Computing Guide for Small-Angle Scattering Experiments*; Institut Laue-Langevin: Grenoble, France, 2006.
(43) Shih, C.-J.; Lin, S.; Strano, M. S.; Blankschtein, D. *J. Am. Chem. Soc.* **2010**, *132*, 14638.
(44) Howard, C. A.; Thompson, H.; Wasse, J. C.; Skipper, N. T. *J. Am. Chem. Soc.* **2004**, *126*, 13228.
(45) Howard, C. A.; Wasse, J. C.; Skipper, N. T.; Thompson, H.; Soper, A. K. *J. Phys. Chem. C* **2007**, *111*, 5640.
(46) Fogden, S.; Howard, C. A.; Heenan, R. K.; Skipper, N. T.; Shaffer, M. S. P. *ACS Nano* **2012**, *6*, 54.
(47) Voiry, D.; Drummond, C.; Pénicaud, A. *Soft Matter* **2011**, *7*, 7998.
(48) Meyer, J. C.; Geim, A. K.; Katsnelson, M. I.; Novoselov, K. S.; Booth, T. J.; Roth, S. *Nature* **2007**, *446*, 60.
(49) Bao, W.; Miao, F.; Chen, Z.; Zhang, H.; Jang, W.; Dames, C.; Lau, C. N. *Nat. Nanotechnol.* **2009**, *4*, 562.